Graphene-based Y-branch laser in femtosecond laser written Nd:YAG waveguides

Hongliang Liu,[1] Chen Cheng,[1] Carolina Romero,[2] Javier R. Vázquez de Aldana,[2] and Feng Chen[1,*]

[1]*School of Physics, State Key Laboratory of Crystal Materials, Shandong University, Jinan 250100, China*
[2]*Laser Microprocessing Group, Universidad de Salamanca, Salamanca 37008, Spain*
[*]*drfchen@sdu.edu.cn*

Abstract: We report on Q-switched waveguide lasers on the graphene-based crystalline Y-branch platform. By applying direct femtosecond laser writing of Nd:YAG laser crystal, a surface waveguide splitter with Y-branch geometry has been fabricated with depressed cladding configuration. The Q-switched lasing operation at 1064 nm is achieved in transmission mode, by attaching a two-layer graphene on the resonator output mirror, as well as by using interaction between the evanescent field and a few-layer graphene that was positioned right above the Y-type waveguide. Q-switched laser with a maximum average power of 173 mW, pulse energy and duration of 63 nJ and 90 ns is obtained. This work opens a way for laser-written crystalline devices as compact, direct-pump laser sources for diverse applications.

OCIS codes: (230.7370) Waveguides; (140.3390) Laser materials processing; (130.3120) Integrated optics devices.

References and links

1. E. K. Mwarania and J. S. Wilkinson, "Modeling of Y-junction waveguide resonators," J. Lightwave Technol. **10**(11), 1700–1707 (1992).
2. E. K. Mwarania, D. M. Murphy, M. Hempstead, L. Reekie, and J. S. Wilkinson, "Integrated Q-switched multiple-cavity glass waveguide laser," IEEE Photon. Technol. Lett. **4**(3), 235–237 (1992).
3. J. Amin, M. Hempstead, J. E. Román, and J. S. Wilkinson, "Tunable coupled-cavity waveguide laser at room temperature in Nd-diffused Ti:$LiNbO_3$," Opt. Lett. **19**(19), 1541–1543 (1994).
4. N. A. Sanford, K. J. Malone, D. R. Larson, and R. K. Hickernell, "Y-branch waveguide glass laser and amplifier," Opt. Lett. **16**(15), 1168–1170 (1991).
5. B. J. Smith, D. Kundys, N. Thomas-Peter, P. G. Smith, and I. A. Walmsley, "Phase-controlled integrated photonic quantum circuits," Opt. Express **17**(16), 13516–13525 (2009).
6. J. C. Cartledge, "Performance of 10 Gb/s lightwave systems based on lithium niobate Mach-Zehnder Modulators with asymmetric Y-branch waveguides," IEEE Photon. Technol. Lett. **7**(9), 1090–1092 (1995).
7. W. Sohler, H. Hu, R. Ricken, V. Quiring, C. Vannahme, H. Herrmann, D. Büchter, S. Reza, W. Grundkötter, S. Orlov, H. Suche, R. Nouroozi, and Y. Min, "Integrated optical devices in lithium niobate," Opt. Photon. News **19**(1), 24–31 (2008).
8. N. Kinrot and M. Nathan, "Investigation of a periodically segmented waveguide Fabry-Pérot interferometer for use as a chemical/biosensor," J. Lightwave Technol. **24**(5), 2139–2145 (2006).
9. Y. Jia, C. Cheng, J. R. Vázquez de Aldana, G. R. Castillo, B. R. Rabes, Y. Tan, D. Jaque, and F. Chen, "Monolithic crystalline cladding microstructures for efficient light guiding and beam manipulation in passive and active regimes," Sci. Rep. **4**, 5988 (2014).
10. J. I. Mackenzie, "Dielectric solid-state planar waveguide lasers: A review," IEEE J. Sel. Top. Quantum Electron. **13**(3), 626–637 (2007).
11. C. Grivas, "Optically pumped planar waveguide lasers, Part I: Fundamentals and fabrication techniques," Prog. Quantum Electron. **35**(6), 159–239 (2011).
12. M. Ams, G. D. Marshall, P. Dekker, J. A. Piper, and M. J. Withford, "Ultrafast laser written active devices," Laser Photonics Rev. **3**(6), 535–544 (2009).
13. F. Chen and J. R. Vázquez de Aldana, "Optical waveguides in crystalline dielectric materials produced by femtosecond-laser micromachining," Laser Photonics Rev. **8**(2), 251–275 (2014).
14. K. Sugioka and Y. Cheng, "Ultrafast lasers-reliable tools for advanced materials processing," Light: Sci. Appl. **3**(4), e149 (2014).
15. R. R. Gattass and E. Mazur, "Femtosecond laser micromachining in transparent materials," Nat. Photonics **2**(4), 219–225 (2008).

#236211 - $15.00 USD Received 16 Mar 2015; revised 31 Mar 2015; accepted 1 Apr 2015; published 7 Apr 2015

16. D. Choudhury, J. R. Macdonald, and A. K. Kar, "Ultrafast laser inscription: perspectives on future integrated applications," Laser Photonics Rev. **8**(6), 827–846 (2014).
17. G. Salamu, F. Jipa, M. Zamfirescu, and N. Pavel, "Laser emission from diode-pumped Nd:YAG ceramic waveguide lasers realized by direct femtosecond-laser writing technique," Opt. Express **22**(5), 5177–5182 (2014).
18. M. T. Hill and M. C. Gather, "Advances in small lasers," Nat. Photonics **8**(12), 908–918 (2014).
19. F. Bonaccorso, Z. Sun, T. Hasan, and A. C. Ferrari, "Graphene photonics and optoelectronics," Nat. Photonics **4**(9), 611–622 (2010).
20. R. R. Nair, P. Blake, A. N. Grigorenko, K. S. Novoselov, T. J. Booth, T. Stauber, N. M. R. Peres, and A. K. Geim, "Fine structure constant defines visual transparency of graphene," Science **320**(5881), 1308 (2008).
21. F. Xia, H. Wang, D. Xiao, M. Dubey, and A. Ramasubramaniam, "Two-dimensional material nanophotonics," Nat. Photonics **8**(12), 899–907 (2014).
22. Y. Ren, G. Brown, R. Mary, G. Demetriou, D. Popa, F. Torrisi, A. C. Ferrai, F. Chen, and A. K. Kar, "7.8 GHz graphene-based 2 μm monolithic waveguide laser," IEEE J. Sel. Top. Quantum Electron. **21**(1), 1602106 (2015).
23. H. Yu, X. Chen, H. Zhang, X. Xu, X. Hu, Z. Wang, J. Wang, S. Zhuang, and M. Jiang, "Large energy pulse generation modulated by graphene epitaxially grown on silicon carbide," ACS Nano **4**(12), 7582–7586 (2010).
24. Q. Bao, H. Zhang, B. Wang, Z. Ni, C. Lim, Y. Wang, D. Tang, and K. P. Loh, "Broadband graphene polarizer," Nat. Photonics **5**(7), 411–415 (2011).
25. Y. Tan, R. He, J. Macdonald, A. K. Kar, and F. Chen, "Q-switched Nd:YAG channel waveguide laser through evanescent field interaction with surface coated graphene," Appl. Phys. Lett. **105**(10), 101111 (2014).
26. J. Siebenmorgen, K. Petermann, G. Huber, K. Rademaker, S. Nolte, and A. Tünnermann, "Femtosecond laser written stress-induced Nd:$Y_3Al_5O_{12}$ (Nd:YAG) channel waveguide laser," Appl. Phys. B **97**(2), 251–255 (2009).

1. Introduction

As the fundamental and significant power division elements in integrated optics, the Y-branch beam splitters based on waveguide platforms have been extensively applied for the development of various photonic devices with a number of advantageous features, such as low propagation loss, ultra-compact volumes and extended cavity configurations [1–3]. Due to the broadband guidance property of optical waveguides and the above advantages, beam splitters combined with conventional optical waveguide have abundant applications on optical telecommunication networks, optical data processing, quantum computing, and biomedical sensing [4–8]. In active media, waveguide lasers act as promising integrated light sources for the construction of monolithically multifunctional photonics systems owing to the low lasing thresholds, comparable laser efficiencies and optimum spatial overlap between pumping source and laser beams [9–11]. In addition to the free-generation regime, the pulsed lasers through the Q-switching and mode-locking have also been achieved in the waveguides based on dielectric materials. To satisfy the requirements to elaborate optical components in advanced materials, the femtosecond laser inscription (FLI) emerged as an efficient and promising three dimensional (3D) photonics device fabrication technology in the past decades [12–16]. Due to the unique feature or flexible 3D micro-engineering, the modification of refractive index at arbitrary depths in the bulks, the FLI technology has been used to produce waveguides with multiple configurations and geometries in dielectric materials [9, 13, 15–17].

The Y-junction splitter, as one kind of remarkable space division multiplexing, benefits the optical communication systems due to its low cost and potential for supporting multiple modes which indeed increases the capacity to meet the enhanced requirement of internet data-processing [6, 18]. Y-branch waveguides have the potential to efficiently combine optical fibers due to the possibility to be inscribed with similar cross-section, thus minimizing the coupling losses. As the significant components of the monolithically integrated optical circuits, Y-branch couplers could be also operated under pulsed conditions with appropriate saturable absorber (SA).

Graphene, due to its exceptional electronic transport properties, has already been shown as promising element in electronic and optical devices in these decades [19–21]. Owing to the zero direct bandgap and broadband wavelength insensitive properties, graphene has been used as SA to realize Q-switched and mode-locked lasers [22, 23]. Meanwhile, the nonlinear absorption of the graphene offers an evanescent field to fulfill pulsed waveguide laser with polarization effect [24, 25]. The Y-branch waveguide lasing have been reported in laser-written photonic structures [9]. In this work, we experimentally achieve the rectangular Y-

#236211 - $15.00 USD Received 16 Mar 2015; revised 31 Mar 2015; accepted 1 Apr 2015; published 7 Apr 2015

branch cladding waveguide beam splitters, which are capable of efficient ultrabroad band wavelength light guiding. Bilayer and multilayer graphene are separately acted as SA by coated on the output mirror and the surface of the transparent material Nd:YAG. Efficient Q-switch laser operation was obtained, in both configurations, using end-pumping at 808 nm with a Ti:Sapphire laser.

2. Experiments in details

The optically polished Nd:YAG crystal (doped by 1 at. % Nd^{3+} ions) used in the work is cut into wafers with dimensions of 10 × 10 × 2 mm^3. A Ti:Sapphire regenerative amplifier (Spitfire, Spectra Physics, USA), which delivers linearly polarized pulses of 120 fs and 795 nm central wavelength with operating at a 1 kHz repetition is utilized as the laser source. The ultrafast laser is focused by a 40 × microscope objective (N.A. ~0.6) and controlled with a mechanical shutter. The pulse energy on the sample is set to 0.6 μJ using a series of optical elements (e.g. a set of half-wave plate, linear polarizing cube, and a calibrated neutral density filter). The femtosecond laser irradiates the sample from the surface of 10 × 10 mm^2 at a constant velocity of 500 μm/s with a 3-μm separation between adjacent two tracks. As shown in Fig. 1(c), the surface Y-branch rectangular cladding waveguide consists of a 6.5-mm length branch section and a 3.5-mm length single section with splitter angle of 0.5° for which the widths of these sections were 25 and 50 μm, respectively. Depths of the cladding waveguides are set to be 50 μm. Microscope images of the input and output faces of the rectangular cladding waveguide are also shown in Fig. 1(c). For comparison, 50-μm-depth straight rectangular cladding waveguide with a width of 50 μm is fabricated under the same conditions.

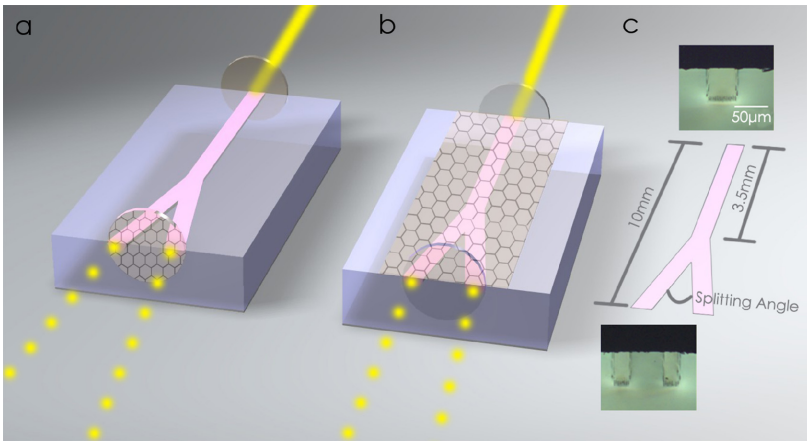

Fig. 1. Experimental setup of Q-switched waveguide laser measurement: (a) bilayer graphene coated on the quartz is adhered to the output face and (b) multilayer graphene coated on the surface of the Y-branch waveguide; (c) schematic diagram of the Y-branch rectangle cladding waveguide and the inset microscope images are the input and the output face of the cladding waveguide.

The pulsed waveguide laser operation experiments are performed by utilizing an end-pumped system. Linearly polarized laser source in the end pumping system at 808 nm is generated from a tunable cw Ti:Sapphire laser (Coherent MBR PE). The polarization of the incident pumping laser is changed by rotation of a half-wave plate. The 808-nm laser is focused to an incident pump laser beam with a waist radius of ~20 μm by a convex lens with focus length of 25 mm. The Fabry-Perot cavity for the 1.06 μm laser emission is formed by placing the resonator mirrors as close as possible to the waveguide surfaces. The input dielectric mirror is with the reflectivity >99% at 1060 ~1065 nm and transmission of ~98% at 800 ~810 nm, and the output one is with reflectivity >99% at 800 ~810 nm and transmission of ~60% at 1060-1065 nm. For Q-switched pulsed laser oscillation operation, there are two

#236211 - $15.00 USD Received 16 Mar 2015; revised 31 Mar 2015; accepted 1 Apr 2015; published 7 Apr 2015

methods of using graphene as SA. Firstly, a bilayer graphene was transferred on the output mirror as shown in Fig. 1(a), and the transmission of the graphene film coated is measured to be 92% at 1064 nm. The bilayer graphene coated on quartz is manufactured by the chemical vapor deposition (CVD) on the copper and nickel disks, and then transferred to the surface of quartz. In the second scheme (Fig. 1(b)), multilayer (6~8 layers) graphene is fabricated with the same technology and transferred to the surface of the Y-branch cladding waveguide. The output lasers from the waveguide's exit face was collected by a 20 × microscope objective (N.A. ~0.4) and imaged by an IR beam profiler through an aperture. We use an oscilloscope (Tektronix TDS 202 2B, 200 MHz) to analyze the pulse trains of the laser beams.

3. Results and discussion

Figures 2(a), 2(b) and 2(e), (2(c), 2(d) and 2(f)) show the Q-switched laser modal profile distributions at 1.06 μm under the 808-nm laser pumping using bilayer graphene deposited on quartz (multilayer graphene on surface). Well-confined fundamental modal profiles collected at both *p* polarization and *s* polarization are demonstrated in the Fig. 2. This feature is consistent with the depressed cladding waveguides in the widely used cubic crystal Nd:YAG, but quite different from the dual-line waveguides produced by ultrafast laser irradiation which only support 1.06-μm laser propagation at *p* polarization [26]. The modal profiles of pulsed laser at *p* polarization are quite different with those at *s* polarization, owing to the polarization dependence absorption of the nanometer-thickness graphene. Figures 2(e) and 2(f) display the average output power of the all-angle 1.06 μm laser in Q-switched and free-generation regimes using bilayer graphene on the output face and multilayer graphene on the surface as SA, respectively. Measurement of the all-angle laser transmission along the transverse plane offers us thorough information of the polarization effects of the guidance. As the circular fitted curve displayed in Fig. 2(e), ~7% difference of the free-generation regime or the Q-switched laser at *p* and *s* polarizations reveals an isotropic light confinement capability. Broadband polarization effect of graphene is double confirmed in Fig. 2(f) with depositing multilayer graphene on the surface of the Y-branch rectangular cladding waveguide. The fitted curve shows that the output powers of the 1.06-μm laser at *p* and *s* polarization are quite different, i.e. at θ = 0° and 180°, the output power of free-generation regime 1064-nm lasers is set to ~80 mW equal to that of Q-switched laser; whereas the corresponding outputs are ~130 mW and ~110 mW at θ = 90° and 270°, respectively. Furthermore, the propagation distance in the graphene-based waveguide also has an influence on the broadband polarization.

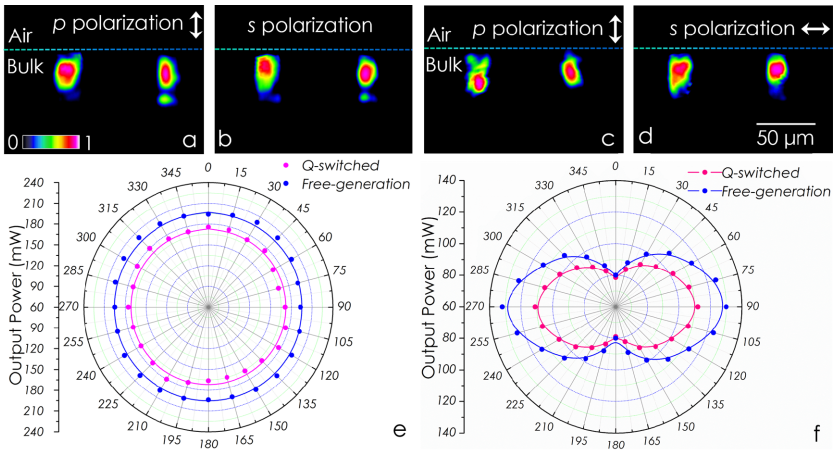

Fig. 2. The measured intensity distributions of the1064-nm waveguide laser at (a) *p* and (b) *s* polarization when the bilayer graphene deposited on the quartz is used; and at (c) *p* and (d) *s* polarization corresponding to the multilayer graphene deposited on the surface of the waveguide. All-angle light transmission along the transverse plane at 1064 nm in the free-generation and Q-switched regimes with using the (e) bilayer graphene and (f) multilayer graphene.

#236211 - $15.00 USD Received 16 Mar 2015; revised 31 Mar 2015; accepted 1 Apr 2015; published 7 Apr 2015

The 1.1-dB/cm propagation loss of the Y-branch rectangle cladding waveguide in free-generation regime is nearly the same with straight waveguide, which proves none additional losses are introduced by the splitter laser cavity and also demonstrates this surface cladding structure is fit for the Q-switched laser oscillation. The output power ration between the two branch sections is 0.51:0.49 for both the laser measurements in Q-switched and free-generation regimes.

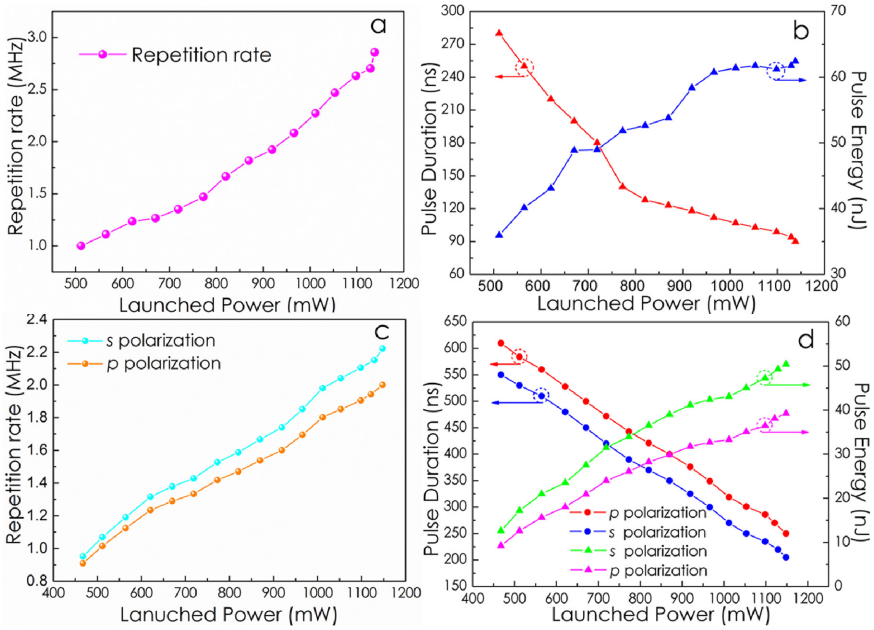

Fig. 3. The features of the pulsed laser at *s* polarization ((a) repetition rate, (b) pulse duration and pulse energy) as functions of the launched power with using the bilayer graphene; the features of the pulsed laser ((c) repetition rate, (d) pulse duration and pulse energy) as functions of the launched power with using the multilayer graphene.

Efficient short-pulse waveguide lasers with pulse energy in scale of nJ and repetition rate in scale of MHz are obtained with the GSA. As displayed in Figs. 3(a) and 3(b), the repetition rate varies from 1.0 MHz to around 3.0 MHz, and the highest pulse energy is 63 nJ when the launched power is about 1150 mW. Meanwhile, the pulse duration decreases from 280 ns to around 90 ns as the launched power decreased to 0.45 W. The differences between the performances of the pulsed laser at *p* and *s* polarizations are less than 7%. Coating multilayer graphene on the surface lead different performances at *p* and *s* polarizations, which is clearly depicted in Figs. 3(c) and 3(d). As a consequence of the evanescent-field interaction between the waveguide laser and the graphene, the Q-switched laser at *p* polarization performs features with lower repetition rate, lower pulse energy and higher pulse duration. The highest repetition rate and pulse energy achieved at *s* polarization is ~2.3 MHz and 50 nJ at launched power of 1.15 W, respectively. Highest repetition rate and pulse energy achieved at *p* polarization is ~2.0 MHz and 40 nJ at the same launched power. The variation of the pulse duration shown in the red line (circular symbol) decrease from 620 ns to 275 ns at lunched power of, which is around 40 ~50 ns larger than the pulse duration of the pulsed laser at *s* polarization shown in blue line (circular symbol). Although distinct from the fully saturate of the broadband polarization reported in the previous work [24], graphene with the evanescent-field interaction design is supposed to be a promising choice for integrated laser source due to its lower cost and the potential to generate stable and shorter-duration pulses with a relatively larger saturation intensity and repetition rate adjustable.

#236211 - $15.00 USD Received 16 Mar 2015; revised 31 Mar 2015; accepted 1 Apr 2015; published 7 Apr 2015

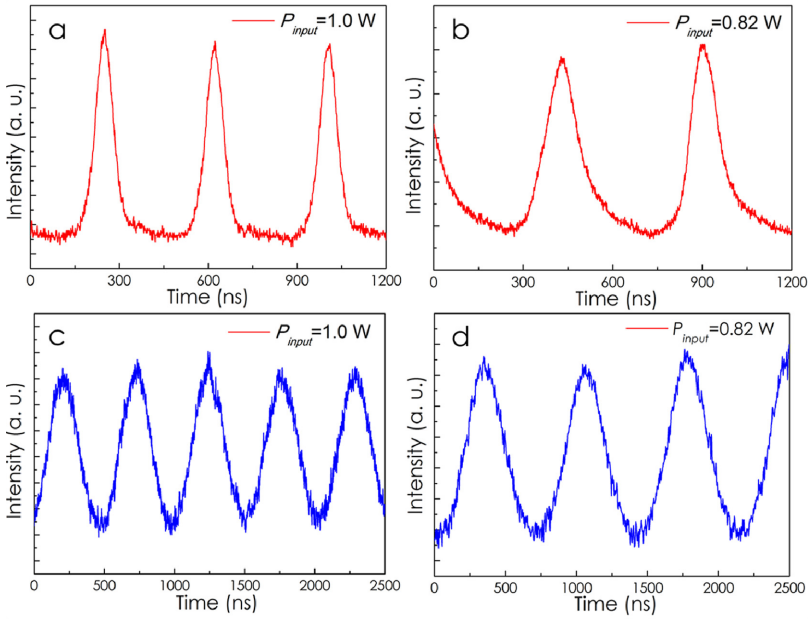

Fig. 4. Pulse trains of the Q-switched waveguide laser obtained with bilayer graphene as SA on the output face when the input power are (a) 1.0 and (b) 0.82 W, respectively; pulse trains of the Q-switched waveguide laser obtained with multilayer graphene as SA on the surface of the waveguide when the input power are (c) 1.0 and (d) 0.82 W, respectively.

Figures 4(a)-4(b) show the pulse trains of the Q-switched waveguide laser with using bilayer graphene SA coated on quartz, and Figs. 4(c)-4(d) depict the pulse trains of the Q-switched waveguide laser with using multilayer graphene coated on the surface of the Y-branch waveguide. The stable pulse train with nearly symmetrical intensity shape also demonstrated the efficient Q-switched short-pulse waveguide laser at nano-second scale generated in the Y-branch waveguide. The pulse duration and the period of the output laser increase along with the launched power decreasing from 1.0 W to 0.82 W obviously, which is quite in good agreement with the previous research about the pulsed waveguide laser [25].

4. Summary

In conclusion, we demonstrate the Q-switched short-pulse laser operation in the Nd:YAG Y-branch waveguide fabricated by ultrafast laser inscription. Few-layer graphene is used as the saturable absorber. The 3.0-MHz Q-switched waveguide laser is obtained with the pulse energy of 63 nJ. Depended on the interaction with the evanescent field of the deposited multilayer graphene, Q-switched waveguide laser with repetition rate of 2.3 MHz and pulse energy of 40 nJ is achieved. Symmetrical Y-branch splitter combined with flexible graphene acting as SA provides coherent pulse Q-switched lasers in MHz band, which opens a direct way for realization of advanced photonics circuits.

Acknowledgments

The work is supported by the National Natural Science Foundation of China (No. 11274203), the Specialized Research Fund for the Doctoral Program of Higher Education of China (No. 20130131130001), and Ministerio de Economía y Competitividad under Project FIS2013-44174-P, Spain.

#236211 - $15.00 USD Received 16 Mar 2015; revised 31 Mar 2015; accepted 1 Apr 2015; published 7 Apr 2015